EurJIC European Journal of Inorganic Chemistry

ChemPubSoc Europe

FULL PAPER

DOI:10.1002/ejic.201300372

Controlled Synthesis of Polyoxopalladates, and Their Gas-Phase Fragmentation Study by Electrospray Ionization Tandem Mass Spectrometry

Zhengguo Lin,[a] Bo Wang,*[a] Jie Cao,[a] Baokuan Chen,[a] Chong Xu,[a] Xianqiang Huang,[a,b] Yanxuan Fan,[a] and Changwen Hu*[a]

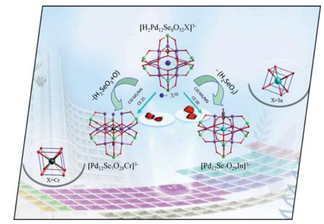

COVER PICTURE

Keywords: Controlled synthesis / Polyoxometalates / Gas-phase fragmentation / Mass spectrometry / Palladium

Two new polyoxopalladates $Na_2H_3[Pd_{12}(\mu_3\text{-}SeO_3)_8(\mu_4\text{-}O)_6(\mu_3\text{-}O)_2Cr]\cdot 25H_2O$ (**1**) and $Na_8H_7[Pd_{12}(\mu_3\text{-}SeO_3)_8(\mu_4\text{-}O)_8In]_3\cdot 24H_2O$ (**2**) have been synthesized by using Cr^{3+} and In^{3+} ions as structural directing agents. The two polyoxopalladates have been characterized by single-crystal X-ray diffraction (SXRD), FTIR and UV/Vis spectroscopy, elemental analysis (EA), ESI-MS, and thermogravimetric analysis (TGA). Detailed SXRD analysis combined with the ESI-MS and a collision-induced dissociation (CID) fragmentation study shows that the coordination configurations of the central ions are different; this affects the stability and fragmentation mechanism of the clusters in the gas phase. This approach may help us to understand the dissociation chemistry and the catalysis mechanism of polyoxopalladates.

Introduction

It is generally acknowledged that conventional polyoxometalates (POMs) as a unique class of metal oxide clusters based on the early transition metals Mo, W, V, Nb, and Ta have provoked significant interest because of their great potential in catalysis, medicine, and electrochemistry.[1] As the active ingredients of many catalysts, noble metals have a wide range of applications in industry.[2,3] Importantly, noble metal atoms can act as the addenda atoms for the construction of a new class of polyanions, which have shown catalytic activity in some organic reactions.[4] During recent years, "unconventional" POMs based on Pt, Pd, and Au have been investigated extensively, and this area of rapid growth has attracted the attention of many chemists.[3–5]

The first noble-metal-based POM, $[Pt_{12}O_8(SO_4)_{12}]^{4-}$, was prepared by the Wickleder group in 2004,[5] and it is worth noting that d^8 noble-metal-based POMs (Pd and Au) have promoted the area after the first polyoxopalladate $[Pd_{13}As_8O_{34}(OH)_6]^{8-}$ was reported by Kortz et al.[6] Several isolated "unconventional" noble-metal-based POMs have been synthesized by hydrolyzation and condensation of noble metal ions (Pd and Au) with oxyacid heterogroups ($PhAsO_3^{2-}$, AsO_4^{3-}, PO_4^{3-}, VO_3^-, or SeO_3^{2-}) in the past four years. For example, the cubical polyanion $[Pd_{13}Se_8O_{32}]^{6-}$,[7] the star-shaped $[Pd_{15}P_{10}O_{50}]^{20-}$,[8] the double-cuboid-shaped $[Cu_2Pd_{22}P_{12}O_{60}(OH)_8]^{20-}$,[9] the first polyoxoaurate $[Au_4As_4O_{20}]^{8-}$,[10] and the largest polyoxopalladate $[Pd_{84}O_{42}(OAc)_{28}(PO_4)_{42}]^{70-}$ wheel cluster[11] were reported. As the heterogroup can terminate the condensation process and allow isolation of the discrete species in the reaction solution,[6] many other polyoxopalladates and polyoxoaurates were prepared by the same approach.[12–16] It is believed that the assembly of these types of clusters is largely affected by hydrolyzation–condensation processes and the selection of various external bridging heterogroups.[6] Very recently, we and the Kortz group successfully incorporated many metal ions in the cavity of the $\{Pd_{12}O_8L_8\}$ shell (L = PO_4^{3-}, $PhAsO_3^{2-}$, $PhPO_3^{2-}$, and SeO_3^{2-}).[17–19] Moreover, we have discovered that guest ions play an important role in the construction of these new palladium-based POMs. The desired polyoxopalladates with a certain structural topology can be prepared by using different metal ions as potential structural directing agents.

Herein, our continued research focuses on the effect of metal ions with various charges and radii in polyoxopalladate synthesis. Furthermore, we sought to investigate their solution stability and gas-phase fragmentations with electrospray ionization tandem mass spectrometry, which may help us to reveal the dissociation chemistry and a feasible catalysis mechanism of the polyoxopalladates. By introducing trivalent transition metal ions (Cr^{3+}) and larger trivalent

[a] Key Laboratory of Cluster Science, Ministry of Education of China, School of Chemistry, Beijing Institute of Technology, Beijing 100081, P. R. China
Fax: +86-10-68912631
E-mail: cwhu@bit.edu.cn
E-mail: bowang@bit.edu.cn
Homepage: http://sc.bit.edu.cn/kyjgjktz/hzwjsktz/index.htm
[b] School of Chemistry & Chemical Engineering, Liaocheng University,
Liaocheng 252059, P. R. China

Supporting information for this article is available on the WWW under http://dx.doi.org/10.1002/ejic.201300372.

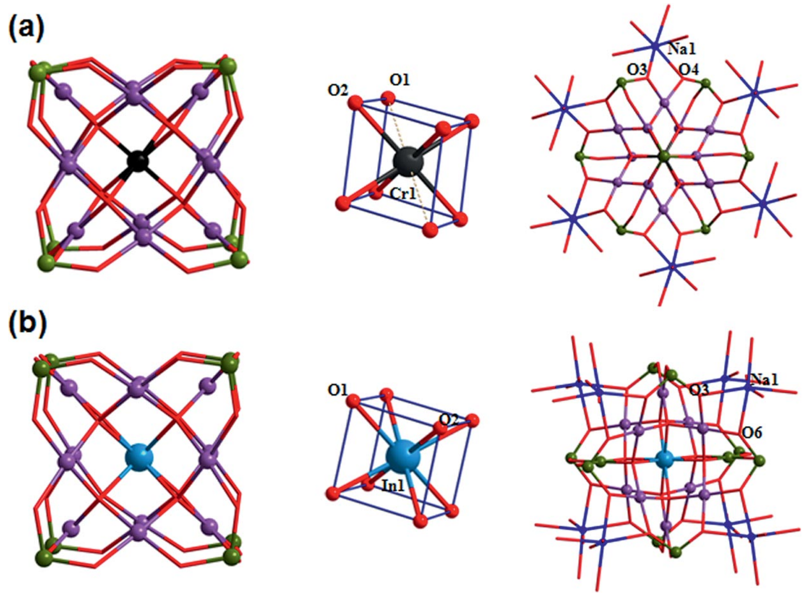

Figure 1. The ball-and-stick and cluster core structures of (a) $[Pd_{12}(\mu_3\text{-}SeO_3)_8(\mu_3\text{-}O)_6(\mu_2\text{-}O)_2Cr]^{5-}$ and (b) $[Pd_{12}(\mu_3\text{-}SeO_3)_8(\mu_3\text{-}O)_8In]^{5-}$. Pd, purple; Se, deep green; O, red; Cr, black; In, cyan; Na, blue.

main group metal ions (In^{3+}) to the polyoxopalladate synthetic reactions, two new cubical polyanions $[Pd_{12}(\mu_3\text{-}SeO_3)_8(\mu_4\text{-}O)_6(\mu_3\text{-}O)_2Cr]^{5-}$ (**1**) and $[Pd_{12}(\mu_3\text{-}SeO_3)_8(\mu_4\text{-}O)_8In]^{5-}$ (**2**, Figure 1) with the typical $\{Pd_{12}\}$ topology were obtained in a one-pot synthesis. Both polyoxopalladates have been characterized by single-crystal X-ray diffraction (SXRD), FTIR and UV/Vis spectroscopy, elemental analysis (EA), and thermogravimetric analysis (TGA). Moreover, their solution stability and gas-phase fragmentation were studied by electrospray ionization tandem mass spectrometry.

Results and Discussion

Crystal Structures and Thermal Stability

The SXRD analysis reveals that the underlying topologies of **1** and **2** resemble those of our previously reported $\{Pd_{12}M^{II}\}$ clusters, and the central M^{2+} ion is replaced by the trivalent metal ions Cr^{3+} and In^{3+}, respectively. In both $\{Pd_{12}X^{III}\}$ clusters, each Pd atom exhibits the expected square-planar geometry and is joined by two "inner" O atoms and two O atoms of a SeO_3^{2-} ion. A truncated cube-shaped shell is then formed by 24 outer O atoms and is capped by eight selenite ions. Compound **1** encompasses a $\{Pd_{12}\}$ cluster shell with a formula of $Na_2H_3[Pd_{12}(\mu_3\text{-}SeO_3)_8(\mu_4\text{-}O)_6(\mu_3\text{-}O)_2Cr]\cdot 25H_2O$ and crystallizes in the trigonal crystal system, space group $R\bar{3}$. Interestingly, the central Cr^{3+} ion is six-coordinate and is bound to six "inner" μ_4-O atoms of the pseudo-cubic body-centered constitution $\{MO_8\}$ (Figure 1, a), which contrasts sharply with the eight-coordinate $M^{II}\text{-}(\mu_4\text{-}O)_8$ cores of the previously reported $\{Pd_{12}M^{II}\}$ clusters.[17] Specifically, the Cr(1)–O(2) bond length in **1** is 2.07 Å, and the other two μ_3-O (O1) atoms of the "inner" distorted cube are 2.53 Å from the central Cr^{3+} ion. This configuration is analogous to that of the $[Pd_{13}Se_8O_{32}]^{6-}$ cluster.[7] The polyanion $[Pd_{12}(\mu_3\text{-}SeO_3)_8(\mu_3\text{-}O)_6(\mu_2\text{-}O)_2Cr]^{5-}$ in crystals linked with six sodium ions forms an interconnected six-membered ring, which then expands into a 2D layer (Figure 2, a).

Compound **2** with a formula of $Na_8H_7[Pd_{12}(\mu_3\text{-}SeO_3)_8(\mu_4\text{-}O)_8\,In]_3\cdot 24H_2O$ also has a $\{Pd_{12}\}$ cluster shell and crystallizes in the cubic crystal system, space group $Pm\bar{3}$. The cluster structural topology of **2** is the same as that of the $\{Pd_{12}M^{II}\}$ clusters (Figure 1, b), and the central In^{3+} ion is coordinated by eight μ_4-O atoms of the $\{InO_8\}$ unit. The eight-coordinate cubic geometry is rare for period 5 elements and only a few examples are known.[20,21] Indeed, compound **2** is the first example in which the main group metal cation is encapsulated in $\{Pd_{12}\}$ cages. The In–O bond lengths in the cluster are 2.22–2.25 Å, and the "inner" μ_4-O atoms serve as cube vertices and are further coordinated by three Pd atoms situated on a trigonal face of the cube. Each polyanion in the crystal of **2** is linked by eight sodium ions at the cube vertices of the cluster and make up an open 3D framework. The square pores of this framework measure approximately 10 Å across based on the largest sphere that could fit into the pores without touching their innermost atoms (blue ball in Figure 2, b).

From the SXRD analyses of the two polyoxopalladates, we noticed that the central ions have different coordination configurations. As previously mentioned, the Cr^{3+} ion in **1** is only six-coordinate and is bound to six "inner" μ_4-O atoms, whereas the In^{3+} ion in **2** is eight-coordinate and is bound to eight "inner" μ_4-O atoms. In contrast, in previously synthesized $\{Pd_{12}M^{II}\}$ clusters, all M^{II} transition metal ions are eight-coordinate. One conceivable explanation is that the Cr^{3+} ion has a smaller ionic radius (0.64 Å) than the In^{3+} ion (0.81 Å), and the different ionic radii can affect the coordination configuration of the metal ions when constructing a certain structure.[21]

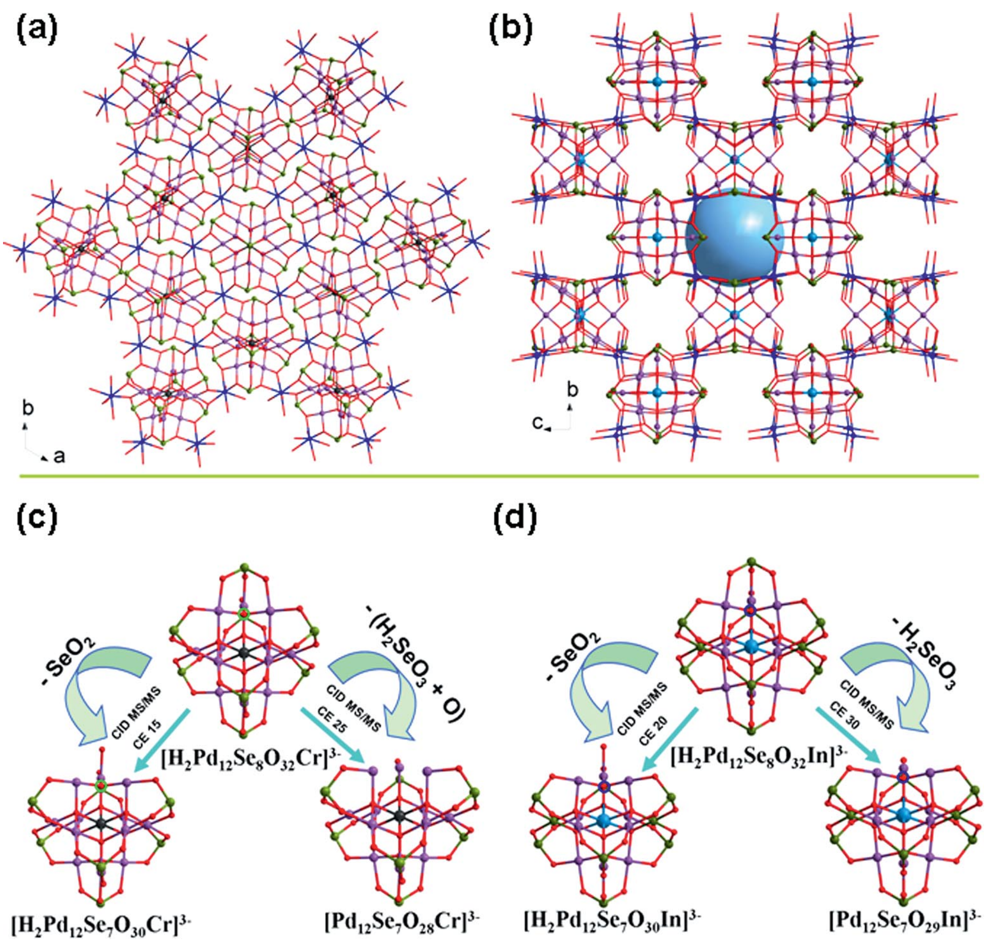

Figure 2. The crystal packing arrangement and the collision-induced dissociation gas-phase fragmentation mechanism of (a and c) $Na_2H_3[Pd_{12}(\mu_3\text{-}SeO_3)_8(\mu_4\text{-}O)_6(\mu_3\text{-}O)_2Cr]\cdot 25H_2O$ and (b and d) $Na_8H_7[Pd_{12}(\mu_3\text{-}SeO_3)_8(\mu_4\text{-}O)_8\ In]_3\cdot 24H_2O$. Pd, purple; Se, deep green; O, red; Cr, black; In, cyan; Na, blue. H atoms are omitted for clarity.

TGA studies of **1** and **2** were performed under N_2 at a rate of 10 °C/min rate (Figure S4a). Three continuous weight losses steps were observed on the TGA curve of **1**. The first weight loss of 7.7% (calcd. 15.1%) in the range 25–230 °C is attributed to the removal of remaining water molecules in the compound, which means the crystal of **1** can easily lose lattice water when exposed to the air. The two-step consecutive weight loss of 28.4% (calcd. 29.8%) covering the temperature range 230–830 °C may be attributed to the release of eight SeO_2 molecules. The TGA curve of **2** is similar to that of **1** (Figure S4b). The first weight loss of 4.9% (calcd. 5.2%) in the range 25–230 °C is attributed to the removal of 24 water molecules, and the two-step consecutive weight loss of 30.9% (calcd. 32.3%) covering the temperature range 230–830 °C may be attributed to the release of 24 SeO_2 molecules.

IR and UV/Vis Spectra

In the IR spectra of **1** and **2** (Figure S2), both compounds show similar characteristic peaks with only slight shifts compared with those of $\{Pd_{12}M^{II}\}$ clusters.[17,18] For **1**, the absorption peaks at 551.3 and 647.3 cm^{-1} may correspond to the Pd–O and Cr–O vibrational modes. The strong peaks at 801.6 and 725.5 cm^{-1} may be attributed to the vibrations of SeO_3 groups. For **2**, the same characteristic peaks and corresponding vibrations can also be found in the IR spectrum. The UV/Vis spectra of **1** and **2** were obtained in the range 190–900 nm. Both compounds also showed similar UV/Vis spectra in the range 200–500 nm with only slight shifts as they have a similar core structure to the $\{Pd_{12}X\}$ clusters (Figure S3). For example, in **1**, the main absorption peaks at 262 nm could be assigned to Pd–O charge-transfer transitions, and the peaks at ca. 320 and 425 nm could be assigned to Pd–Pd electron-induced transitions and d–d electronic transition of Pd^{2+}.

ESI-MS Spectra and Gas-Phase Fragmentation

In recent years, ESI-MS has been used as a versatile tool for the characterization of the detailed structures of complex inorganic POM clusters,[22,23] and many gas-phase fragmentation reactions of POM anions have been studied by collision-induced dissociation (CID) MS/MS.[24] To investigate whether the different coordination configurations of the central ions can affect the stability and dissociation chemistry of **1** and **2**, we studied their stability and gas-phase fragmentation reactions by ESI tandem mass spectrometry (Figures 3 and 4). The general strategy includes assignment of the polyanion species, determination of the stability of the clusters in the gas phase, and elucidation of the dissociation mechanism. The mass spectra were recorded with an Agilent 6520 Q-TOF LC/MS mass spectrometer, and all experiments were performed in negative mode by direct injection. The CID fragmentation experiments of the desired multiple-charged cluster were performed by using N_2 as the target gas, and the desired parent anions were isolated and subjected to energy-variable collision-induced dissociation.

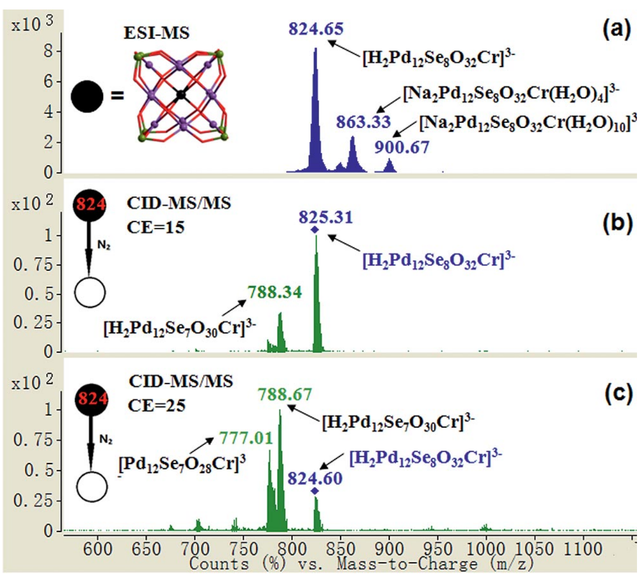

Figure 3. Negative ion mass spectrum of $Na_2H_3[Pd_{12}(\mu_3\text{-}SeO_3)_8(\mu_4\text{-}O)_6(\mu_3\text{-}O)_2Cr]\cdot 25H_2O$ dissolved in 1:1 H_2O/CH_3CN (a) and CID–MS/MS spectra of $[H_2Pd_{12}(\mu_3\text{-}SeO_3)_8(\mu_4\text{-}O)_6(\mu_3\text{-}O)_2Cr]^{3-}$ under the collision energy (CE) voltages of 15 (b) and 25 V (c).

For **1**, the ESI-MS spectrum (Figure 3, a) shows that the major peaks observed can be assigned to polyanion species related to the $\{Pd_{12}Cr\}$ cluster. The peak centered at m/z = 824.65 can be assigned to the triply negatively charged diprotonated cluster $[H_2Pd_{12}Se_8O_{32}Cr]^{3-}$, the peak at m/z = 863.33 can be assigned to $[Na_2Pd_{12}Se_8O_{32}Cr(H_2O)_4]^{3-}$, and the peak at m/z = 900.67 can be assigned to $[Na_2Pd_{12}Se_8O_{32}Cr(H_2O)_{10}]^{3-}$. In subsequent gas-phase fragmentation, we selected the $[H_2Pd_{12}Se_8O_{32}Cr]^{3-}$ cluster as the parent anion (marked with a blue square in Figure 3, b and c) and subjected it to collision-induced Coulomb explosion dissociation under the collision energy (CE) voltages of 15 and 20 V. This parent anion displays an interesting fragmentation pathway to generate different product anions. As the CID–MS/MS spectrum in Figure 3 (b) shows, $[H_2Pd_{12}Se_8O_{32}Cr]^{3-}$ mostly generated $[H_2Pd_{12}Se_7O_{30}Cr]^{3-}$ (m/z = 788.34) and SeO_2 at 15 V. At a CE voltage of 25 V, both $[H_2Pd_{12}Se_7O_{30}Cr]^{3-}$ (m/z = 788.67) and $[Pd_{12}Se_7O_{28}Cr]^{3-}$ (m/z = 777.01) can be generated by the parent ions, which means that SeO_2 or H_2SeO_3 plus an O atom dissociates from the parent anion (Figure 3, c). Indeed, some small product anions such as $[SeO_2]^-$ and $[HSeO_3]^-$ can be observed in the CID–MS/MS spectrum (Figure S5).

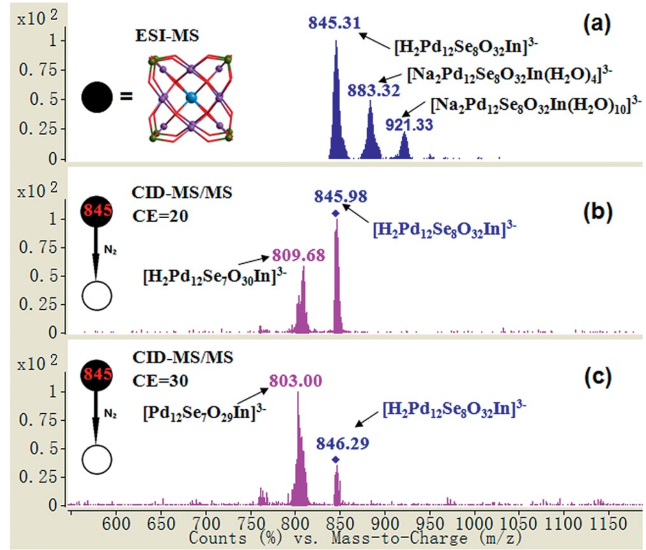

Figure 4. Negative ion mass spectrum of $Na_8H_7[Pd_{12}(\mu_3\text{-}SeO_3)_8(\mu_4\text{-}O)_8In]_3\cdot 24H_2O$ dissolved in 1:1 H_2O/CH_3CN (a) and CID–MS/MS spectra of $[H_2Pd_{12}(\mu_3\text{-}SeO_3)_8(\mu_4\text{-}O)_8In]^{3-}$ under the CE voltages of 20 (b) and 30 V (c).

In the ESI-MS spectrum of **2** (Figure 4, a), the major peaks are strikingly similar to those of **1**. The peak centered at m/z = 845.31 can be assigned to the triply negatively charged diprotonated cluster $[H_2Pd_{12}Se_8O_{32}In]^{3-}$, the peak at m/z = 883.32 can be assigned to $[Na_2Pd_{12}Se_8O_{32}In(H_2O)_4]^{3-}$, and the peak at m/z = 921.33 can be assigned to $[Na_2Pd_{12}Se_8O_{32}In(H_2O)_{10}]^{3-}$. In the same way, we selected the $[H_2Pd_{12}Se_8O_{32}In]^{3-}$ cluster as the parent anion (marked with a blue square in Figure 4b and c), which was dissociated at 20 V. The CID MS/MS spectrum showed that the $[H_2Pd_{12}Se_8O_{32}In]^{3-}$ mostly generated $[H_2Pd_{12}Se_7O_{30}In]^{3-}$ (m/z = 809.68, Figure 4, b). At a CE voltage of 30 V, the dissociation mechanism of **2** started to differ from that of **1**. Specifically, the main product ions generated by the parent anion are $[Pd_{12}Se_7O_{29}In]^{3-}$ (m/z = 803.00) or $[H_2Pd_{12}Se_7O_{30}In]^{3-}$ (m/z = 809.68), which can only be attributed to the dissociation of one H_2SeO_3 or SeO_2 molecule from the parent anion. The related fragment species can also be observed in the CID–MS/MS spectrum (Figures 4, c and S6).

As expected, both polyoxopalladates maintain intact cluster structures in solution and the gas phase. Furthermore, it is notable that the CID fragmentation reaction of the selected parent anion $[H_2Pd_{12}Se_8O_{32}X]^{3-}$ (X = Cr and In) undergoes the same dissociation mode in a low-energy collision-induced dissociation, whereas different dissociations mode are observed at higher energy (Figure 2, c and d). When the parent anions are dissociated at low energy (15 and 20 V for **1** and **2**, respectively), they both strip off a SeO_2 molecule. However, at higher energy, the fragmentation species leaving $[H_2Pd_{12}Se_8O_{32}Cr]^{3-}$ is different from that leaving $[H_2Pd_{12}Se_8O_{32}In]^{3-}$. One additional O atom is dissociated from $[H_2Pd_{12}Se_8O_{32}Cr]^{3-}$ in addition to a species related to a H_2SeO_3 molecule, although the CE voltage of $[H_2Pd_{12}Se_8O_{32}Cr]^{3-}$ (25 V) is lower than that of $[H_2Pd_{12}Se_8O_{32}In]^{3-}$ (30 V). From the SXRD analyses of these two compounds, we have learned that the central metal ions encapsulated in the parent anions $[H_2Pd_{12}Se_8O_{32}X^{III}]^{3-}$ (X = Cr and In) show different coordination configuration. The Cr^{3+} ion is only coordinated to six "inner" μ_4-O atoms in **1**, whereas the In^{3+} ion is coordinated to eight "inner" μ_4-O atoms in **2**. Two μ_3-O atoms of the pseudo-cubic body-centered $\{CrO_8\}$ unit are not bonded with the central Cr^{3+} ion, which means they can easily dissociate from the cluster. In the CID fragmentation experiments, the parent anion $[H_2Pd_{12}Se_8O_{32}Cr]^{3-}$ can release a SeO_2 molecule at low CE. At higher CE, after a SeO_3^{2-} ion leaves the vertex of the intact parent anion, an additional μ_3-O atom (marked with a green circle, Figure 2, c) dissociates from the cluster. In comparison, the eight-coordinate In^{3+} ion in **2** is tightly bonded to eight μ_4-O atoms; therefore, only a SeO_3^{2-} ion dissociates from $[H_2Pd_{12}Se_8O_{32}In]^{3-}$ (Figure 2, d) even at higher energy (30 V). This result along with the SXRD data suggests that the coordination configuration of the central metal ions affects the cluster stability and dissociation chemistry of polyoxopalladates. Furthermore, this innovative approach can also help us to understand the relationship between the stability and structural diversity of various polyoxopalladates.

Conclusions

By introducing metal ions X (Cr^{3+} and In^{3+}) with the same charge but different radii as structural directing agents, we have successfully synthesized two new cubical $\{Pd_{12}X^{III}\}$ polyoxopalladates, namely, $[Pd_{12}(\mu_3\text{-}SeO_3)_8(\mu_4\text{-}O)_6(\mu_3\text{-}O)_2Cr]^{5-}$ (**1**) and $[Pd_{12}(\mu_3\text{-}SeO_3)_8(\mu_4\text{-}O)_8In]^{5-}$ (**2**). Detailed SXRD analyses combined with ESI-MS and a CID fragmentation study reveal that the central cation plays a critical role in the structural configuration formation and the structural stability of the two polyoxopalladates. Specifically the Cr^{3+} ion is coordinated to six "inner" μ_4-O atoms in **1**, and the In^{3+} ion is coordinated to eight "inner" μ_4-O atoms in **2**. In addition, for the first time, we studied their solution stability and gas-phase fragmentations with electrospray ionization tandem mass spectrometry and investigated the dissociation mechanism of the two compounds. The results show that the coordination configurations of the metal center can affect the stability and gas-phase fragmentation mechanism of the clusters, which may help us to understand the dissociation chemistry and the catalysis mechanism of polyoxopalladates.[25]

Experimental Section

Materials and General Methods: All reagents were purchased from commercial sources and used without further purification. Elemental analysis was performed with a Perkin–Elmer Elan 6100 ICP-MS. IR spectra were recorded in the range 4000–400 cm^{-1} with a Nicolet 170SX-FT/IR spectrometer by using samples as KBr pellets. The UV/Vis spectra were obtained with a TU-1901 spectrophotometer in the range 200–900 nm. The TGA was performed under a N_2 atmosphere from room temperature to 1000 °C at a heating rate of 10 °C/min with a DTG-60AH instrument. Mass spectra measurements were made in the negative ion mode with an Agilent 6520 Q-TOF LC/MS mass spectrometer coupled to an Agilent 1200 LC system. Sample solutions were ca. 10^{-5} M in water and were transferred to the electrospray source by direct injection. The CID fragmentation experiments were performed with N_2 as the target gas, and the desired parent anion was isolated and subjected to CE variable collision-induced dissociation.

$Na_2H_3[Pd_{12}(\mu_3\text{-}SeO_3)_8(\mu_4\text{-}O)_6(\mu_3\text{-}O)_2Cr]\cdot 25H_2O$ (1): SeO_2 (0.033 g, 0.3 mmol), $Pd(OAc)_2$ (0.067 g, 0.3 mmol), and $CrCl_3$ (0.0158 g, 0.1 mmol) were dissolved in NaOAc/AcOH buffer (10 mL, 0.5 M, pH 5.0). This solution was stirred and heated to 50 °C for 3 h. The red-brown solution was then cooled to room temperature, and the small amount of precipitate was removed by filtration. The resulting solution was left to evaporate. After several weeks, deep red-brown block-shaped crystals of suitable quality for single-crystal X-ray diffraction were obtained (yield based on Pd: 23 %). Selected IR (KBr): $\tilde{\nu}$ = 1618.1 (m), 1383.9 (w), 1128. 7 (w), 801.6 (s), 725.5 (s), 647.3 (w), 551.3 (s), 507.97 (w) cm^{-1}. $CrH_{53}Na_2O_{57}Pd_{12}Se_8$ (2971.82): calcd. Cr 1.75, Na 1.54, Pd 42.97, Se 21.25; found Cr 1.64, Na 1.62, Pd 41.07, Se 21.13.

$Na_8H_7[Pd_{12}(\mu_3\text{-}SeO_3)_8(\mu_4\text{-}O)_8\ In]_3\cdot 24H_2O$ (2): SeO_2 (0.033 g, 0.3 mmol), $InCl_3$ (0.0221 g, 0.1 mmol), and $Pd(OAc)_2$ (0.067 g, 0.3 mmol) were dissolved in NaOAc/AcOH buffer (10 mL, 0.5 M, pH 5.0). This solution was stirred and heated to 50 °C for 2.5 h. The red-brown solution was cooled to room temperature, and the small amount of precipitate was removed by filtration. The resulting solution was left to evaporate. After several days, red-brown block-shaped crystals of suitable quality for single-crystal X-ray diffraction were obtained (yield based on Pd: 61 %). Selected IR (KBr): $\tilde{\nu}$ = 1636.8 (m), 1560.81 (m), 1410.5 (w), 1384.6 (w), 1046.6 (w), 794.6 (s), 724.8 (s), 645.4 (w), 552.2 (s), 530. 7 (w) cm^{-1}. $H_{55}In_3Na_8O_{120}Pd_{36}Se_{24}$ (8229.36): calcd. In 4.18, Na 2.23, Pd 46.55, Se 23.02; found In 4.03, Na 2.41, Pd 45.82, Se 22.61.

X-Ray Crystallography: The crystal data for **1** and **2** were collected at 120(2) K with a Bruker APEX–II CCD diffractometer with graphite monochromatic Mo-K_α radiation (λ = 0.71073 Å). Crystals were mounted on a glass fiber and fixed with glue. All structures were solved by direct methods and refined by full-matrix least-squares against Fo^2 by the *SHELXTL* program package (Bruker).[26,27] The active hydrogen atoms were not incorporated in the refinement, and all atoms were refined anisotropically. The crystallographic details and the selected bond lengths of the two compounds are summarized in Tables S1 and S2. Further details on the crystal structure investigations may be obtained from the Fachinformationszentrum Karlsruhe, Germany, 76344 Eggenstein-Leopoldshafen, Germany (fax: +49-7247-808-666; e-mail: crysdata@fiz-karlsruhe.de), on quoting the depository numbers CSD-425693 (**1**), CSD-425694 (**2**).

Supporting Information (see footnote on the first page of this article): ORTEP drawings of the anionic parts of **1** and **2** (Figure S1). The IR (Figure S2), UV (Figure S3), TGA (Figure S4), and CID MS/MS spectra (Figure S5 and S6) of **1** and **2**. The crystallographic details and the selected bond lengths of **1** and **2** (Tables S1 and S2).

Acknowledgments

The authors are grateful to the National Natural Science Foundation of China (NSFC) (grant numbers 21173021, 21231002, 21276026), the 111 Project (grant number B07012), and the Program of Cooperation of the Beijing Education Commission (grant number 20091739006).

[1] a) M. T. Pope, *Heteropoly and Isopoly Oxometalates*, Springer, Berlin, **1983**, p. 1–87; b) C. L. Hill (Ed.), *Chem. Rev.* **1998**, *98*, 1–390; c) T. Yamase, M, T. Pope, *Polyoxometalate Chemistry for Nano-Composite Design*, Kluwer Academic Publishers, New York, **2002**, p. 1–114; d) D. L. Long, R. Tsunashima, L. Cronin, *Angew. Chem.* **2010**, *122*, 1780–1803; *Angew. Chem. Int. Ed.* **2010**, *49*, 1736–1758; e) U. Kortz, A. Müler, J. V. Slageren, J. Schnack, N. S. Dalal, M. Dressel, *Coord. Chem. Rev.* **2009**, *253*, 2315–2327.

[2] a) G. Ertl, J. Weitkamp, *Handbook of Heterogeneous Catalysis*, Wiley, Weinheim, Germany **2008**, p. 1–207; b) I. W. C. E. Arends, G. J. T. Brink, R. A. Sheldon, *Science* **2000**, *287*, 1636–1639; c) M. S. Sigman, D. R. Jensen, *Acc. Chem. Res.* **2006**, *39*, 221–229.

[3] a) W. H. Knoth, P. Domaille, R. L. Harlow, *Inorg. Chem.* **1986**, *25*, 1577–1584; b) L. H. Bi, U. Kortz, B. Keita, L. Nadjo, H. Borrmann, *Inorg. Chem.* **2004**, *43*, 8367–8372; c) P. Putaj, F. Lefebvre, *Coord. Chem. Rev.* **2011**, *255*, 1642–1685.

[4] N. V. Izarova, M. T. Pope, U. Kortz, *Angew. Chem. Int. Ed.* **2012**, *51*, 9492–9510.

[5] M. Pley, M. S. Wickleder, *Angew. Chem.* **2004**, *116*, 4262–4264; *Angew. Chem. Int. Ed.* **2004**, *43*, 4168–4170.

[6] E. V. Chubarova, M. H. Dickman, B. Keita, L. Nadjo, F. Miserque, M. Mifsud, I. W. C. E. Arends, U. Kortz, *Angew. Chem.* **2008**, *120*, 9685; *Angew. Chem. Int. Ed.* **2008**, *47*, 9542–9546.

[7] N. V. Izarova, M. H. Dickman, R. Ngo Biboum, B. Keita, L. Nadjo, V. Ramachandran, N. S. Dalal, U. Kortz, *Inorg. Chem.* **2009**, *48*, 7504–7506.

[8] N. V. Izarova, R. Ngo Biboum, B. Keita, M. Mifsud, I. W. C. E. Arends, G. B. Jameson, U. Kortz, *Dalton Trans.* **2009**, 9385–9387.

[9] M. B. Stuckart, N. V. Izarova, G. B. Jameson, V. Ramachandran, Z. X. Wang, J. V. Tol, N. S. Dalal, R. N. Biboum, B. Keita, L. Nadjo, U. Kortz, *Angew. Chem.* **2011**, *123*, 2688–2692; *Angew. Chem. Int. Ed.* **2011**, *50*, 2639–2642.

[10] N. V. Izarova, N. Vankova, T. Heine, R. N. Biboum, B. Keita, L. Nadjo, U. Kortz, *Angew. Chem.* **2010**, *122*, 1930–1933; *Angew. Chem. Int. Ed.* **2010**, *49*, 1886–1889.

[11] F. Xu, H. N. Miras, R. A. Scullion, D. L. Long, J. Thiel, L. Cronin, *Proc. Natl. Acad. Sci. USA* **2012**, *109*, 11609–11612.

[12] M. Barsukova, N. V. Izarova, R. Ngo Biboum, B. Keita, L. Nadjo, V. Ramachandran, N. S. Dalal, N. S. Antonova, J. J. Carbó, J. M. Poblet, U. Kortz, *Chem. Eur. J.* **2010**, *16*, 9076–9085.

[13] M. Delferro, C. Graiff, L. Elviri, G. Predieri, *Dalton Trans.* **2010**, *39*, 4479–4481.

[14] N. V. Izarova, N. Vankova, A. Banerjee, G. B. Jameson, T. Heine, F. Schinle, O. Hampe, U. Kortz, *Angew. Chem.* **2010**, *122*, 7975–7980; *Angew. Chem. Int. Ed.* **2010**, *49*, 7807–7811.

[15] F. Xu, R. A. Scullion, J. Yan, H. N. Miras, C. Busche, A. Scandurra, B. Pignataro, D. L. Long, L. Cronin, *J. Am. Chem. Soc.* **2011**, *133*, 4684–4686.

[16] Y. X. Xiang, N. V. Izarova, F. Schinle, O. Hampe, B. Keita, U. Kortz, *Chem. Commun.* **2012**, *48*, 9849–9851.

[17] Z. G. Lin, B. Wang, J. Cao, B. K. Chen, Y. Z. Gao, Y. N. Chi, C. Xu, X. Q. Huang, R. D. Han, S. Y. Su, C. W. Hu, *Inorg. Chem.* **2012**, *51*, 4435–4437.

[18] M. Barsukova-Stuckart, N. V. Izarova, R. Barrett, Z. Wang, J. van Tol, H. W. Kroto, N. S. Dalal, B. Keita, D. Heller, U. Kortz, *Chem. Eur. J.* **2012**, *18*, 6167–6171.

[19] M. B. Stuckart, N. V. Izarova, R. A. Barrett, Z. X. Wang, J. van Tol, H. W. Kroto, N. S. Dalal, P. J. Lozano, J. J. Carbo, J. M. Poblet, M. S. von Gernler, T. Drewello, P. de Oliveira, B. Keita, U. Kortz, *Inorg. Chem.* **2012**, *51*, 13214–13228.

[20] S. T. Zheng, J. T. Bu, Y. F. Li, T. Wu, F. Zuo, P. Y. Feng, X. H. Bu, *J. Am. Chem. Soc.* **2010**, *132*, 17062–17064.

[21] a) R. D. Shannon, *Acta Crystallogr., Sect. B* **1969**, *25*, 925–946; b) R. D. Shannon, C. T. Prewitt, *Acta Crystallogr., Sect. A* **1976**, *32*, 751–767.

[22] a) T. Ito, T. Yamase, *Eur. J. Inorg. Chem.* **2009**, 5205–5210; b) H. N. Miras, J. Yan, D. L. Long, L. Cronin, *Angew. Chem.* **2008**, *120*, 8548–8551; *Angew. Chem. Int. Ed.* **2008**, *47*, 8420–8423; c) L. V. Nadal, A. R. Fortea, L. K. Yan, E. F. Wilson, L. Cronin, J. M. Poblet, *Angew. Chem.* **2009**, *121*, 5560–5564; *Angew. Chem. Int. Ed.* **2009**, *48*, 5452–5456; d) M. J. Deery, O. W. Howarth, K. R. Jennings, *J. Chem. Soc., Dalton Trans.* **1997**, 4783–4788; e) H. N. Miras, E. F. Wilson, L. Cronin, *Chem. Commun.* **2009**, 1297–1311.

[23] a) P. J. Robbins, A. J. Surman, J. Thiel, D. L. Long, L. Cronin, *Chem. Commun.* **2013**, *49*, 1909–1911; b) H. N. Miras, H. Y. Zang, D. L. Long, L. Cronin, *Eur. J. Inorg. Chem.* **2011**, 5105–5111; c) J. Yan, D. L. Long, E. F. Wilson, L. Cronin, *Angew. Chem.* **2009**, *121*, 4440–4444; *Angew. Chem. Int. Ed.* **2009**, *48*, 4376–4380; d) D. L. Long, C. Streb, Y. F. Song, S. Mitchell, L. Cronin, *J. Am. Chem. Soc.* **2008**, *130*, 1830–1832.

[24] a) R. Llusar, I. Sorribes, C. Vicent, *J. Cluster Sci.* **2009**, *20*, 177–192; b) J. Cao, C. C. Li, Z. X. Zhang, C. Xu, J. Yan, F. Y. Cui, C. W. Hu, *J. Am. Soc. Mass Spectrom.* **2012**, *23*, 366–374; c) T. H. Bray, R. Copping, D. K. Shuh, J. K. Gibson, *Int. J. Mass Spectrom.* **2011**, *299*, 35–46.

[25] J. C. Goloboy, W. G. Klemperer, *Angew. Chem.* **2009**, *121*, 3614–3614; *Angew. Chem. Int. Ed.* **2009**, *48*, 3562–3564.

[26] G. M. Sheldrick, *SHELXL 97*, *Program for the Refinement of Crystal Structures*, University of Göttingen, Germany, **1997**.

[27] G. M. Sheldrick, *SHELXTL NT/2000*, v. 6.12, Bruker Analytical X-ray Systems, Madison, WI.

Received: March 19, 2013
Published Online: May 21, 2013

